



VELOCITY MEASUREMENTS IN THE NEAR WAKE OF A MODEL ROTOR
AND COMPARISON WITH THEORETICAL RESULTS

BY

N.J. VERMEER AND G.J.W. VAN BUSSEL

INSTITUTE FOR WINDENERGY
DELFT UNIVERSITY OF TECHNOLOGY
DELFT, THE NETHERLANDS

FIFTEENTH EUROPEAN ROTORCRAFT FORUM

SEPTEMBER 12 - 15, 1989 AMSTERDAM

VELOCITY MEASUREMENTS IN THE NEAR WAKE OF A MODEL ROTOR
AND COMPARISON WITH THEORETICAL RESULTS

N.J. VERMEER AND G.J.W. VAN BUSSEL

INSTITUTE FOR WINDENERGY
DELFT UNIVERSITY OF TECHNOLOGY
DELFT, THE NETHERLANDS

ABSTRACT

In a research program for output optimization of horizontal axis windturbines, preliminary velocity measurements in the wake of a small-scale model have been performed in an open-jet wind tunnel. By taking velocity samples of a hot wire every 0.5° azimuth angle of the rotor, the influence of bound vorticity, vorticity sheet and tipvortex can be distinguished clearly. From reduced data of the axial traverses, the circulation on the rotating blade can be obtained.

A comparison, concerning the circumferential variation of the axial velocity and blade loads, has been made with the computer codes VIAX and PREDICHAT, which are based on the acceleration potential method. The comparison is carried out in a qualitative way, but shows basically the same phenomena as in the experiments. It also shows that the proposed procedure to estimate local blade circulation from the measured axial velocity variation is very promising.

NOTATION

c	chord	m
C_P	power coefficient: $P / (\frac{1}{2} \rho U^3 \pi R^2)$	-
C_D	axial force coefficient: $D_{ax} / (\frac{1}{2} \rho U^2 \pi R^2)$	-
Cl^{ax}	lift curve slope: $dCl/d\alpha$	-
D_{ax}	axial force	N
P^{ax}	nett power at the axis	Nm/s
r	radial coordinate	m
R	radius	m
U	tunnel wind velocity	m/s
V_1	velocity measured by front wire	m/s
V_2	velocity measured by hind wire	m/s
ΔV	velocity fluctuation	
	by blade passage	m/s
z	axial coordinate	m
Ω	rotational speed	rad/s
Γ	circulation	m^2/s
λ	tip-speed ratio: QR/U	-
θ_{tip}	pitch-angle at blade tip	degrees
ψ	azimuth angle	degrees

1. INTRODUCTION

Most computer-codes for predicting rotor loads and energy output of windturbines use the 2-dimensional aerofoil characteristics in a blade-element momentum approach. Empirical corrections are used to incorporate possible 3-dimensional effects for the rotating situation. In spite of these corrections, performance predictions are still not very accurate and load predictions are even worse (fig. 1), even at the optimum setting of the pitch-angle.

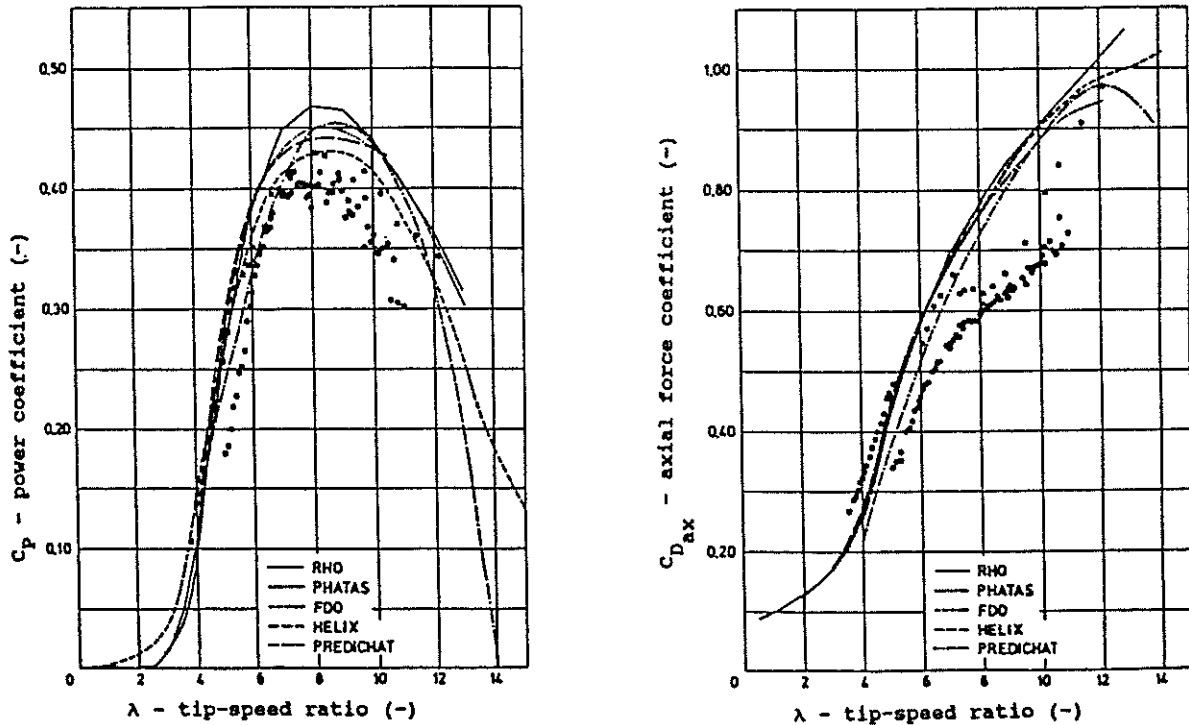


Figure 1. Comparison of field test and predictions

This is shown in a Dutch workshop on rotor aerodynamics of horizontal axis windturbines, reported by Van Bussel and Van Kuik [1]. In this workshop the 25m HAT at Petten was used as a testcase to compare 5 prediction codes with each other and with measurements. When the considered codes are applied to an increased setting of the pitch-angle, what works out as a smaller induced velocity, the predictions get worse. This indicates a lack of physical insight to describe the operational situation sufficiently.

Aerofoil lift and drag coefficients obtained from wind tunnel measurements only express the global influence on the flow. The considered aerofoil is 2-dimensional and the oncoming flow is uniform. As a wind turbine blade an aerofoil is subject to: 3-dimensionality, rotation, energy extraction and wake expansion. There is by no means enough knowledge of such a situation to extract any reliable correction factors for the section lift and drag coefficients to represent these conditions. Wake measurements are mainly performed at a few diameters distance from the rotor plane for interference models for park situations. Only recently Clausen and Wood [2] performed some detailed flow measurements in the wake of a model rotor to

investigate the discrepancies between mean flow measurements and blade element theory (see Clausen et al. [3]).

For a better understanding of the complex flow around a rotor, an experimental set-up has been realized to measure the instantaneous velocities in the wake of a rotating model. Special attention is paid to the near-wake.

2. APPARATUS

2.1 Windtunnel

The measurements have been performed in the open-jet wind tunnel of the Institute for Windenergy. This tunnel consists of a straight circular flowchannel, with a fan at the inlet, gauzes and a flow-straightener. The diameter is 2.24 m. The turbulence level is approximately 1%. The velocity uniformity over the total outlet area is not very well, but an area is chosen over which the maximum deviation from the average velocity is 2%.

2.2 Model

As a model the T.H.E. 2-4-20 rotor (fig. 2) has been used, which has the following properties:

Number of blades : 2, with curved-plate aerofoil sections

Radius : 0.1 m

Blade-taper : $c/R = 0.284 - 0.162r/R$ ($0.3 < r/R < 1$)

Blade-twist : $\theta = (18.2 + \theta_{\text{tip}}) - 18.2r/R$ (in degrees)

Performance at $\lambda = 5.1$:

θ_{tip}	C_P	$C_{D_{ax}}$
+1.3°	0.27	0.63
-2.7°	0.23	0.85

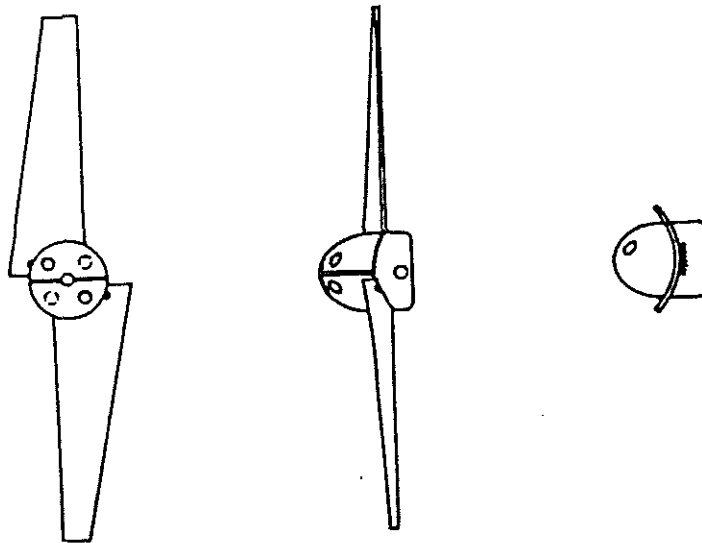


Figure 2. The T.H.E. 2-4-20 rotor model

The blades are secured in slits in the hub, thus providing the possibility to change the pitch-angle.

A mini-motor has been used as generator. It is fixed to the rotor through a flexible attachment, to reduce torque losses by misalignment.

On the axis an opto-coupler is installed to detect the speed of revolutions. This is also used to determine the azimuthal position of the rotor.

The external load, to control the speed of revolutions, is applied by means of a decade resistance instrument.

The torque of the generator has been calibrated as a function of load and rotational speed and also the torque losses in the bearings have been calibrated as a function of rotational speed. In this way the net-power at the axis can be determined. The axial force on the blades has been determined by mounting the model via a pole on a torsion axis. The influence of generator and hub has been taken into account. Flow visualization with smoke showed a large separation area near the hub. This high thrust is partly caused by a high local solidity and contributes in an unequal way to the total thrust. This is confirmed by visualization of the wake expansion, which is indirectly also a measure of the total thrust. The expansion was not according to the measured thrust.

2.3 Instrumentation

The undisturbed velocity is measured with a Pitot-tube connected to a Betz-manometer. This Pitot-tube is placed in such a way that it represents the average velocity over the above described test area.

The wake velocities are measured with constant temperature hot-wire equipment. The cross-wires are perpendicular to each other and both parallel with the rotor plane. The front wire is orientated in span (radial) direction and measures the resultant of axial and tangential velocities; the hind wire is orientated in chord (tangential) direction and measures the resultant of axial and radial velocities.

The probe is positioned by a traverse system. In radial direction the absolute error is 0.2 mm. In axial direction the absolute error is 2 mm (the exact position of the rotor plane is difficult to detect and dangerous for the probe too), but the incremental error is 0.2 mm.

A data acquisition system, containing a high-speed voltmeter and a multiplexer, is used to measure and store the signals of the hot-wires and a revolution counter.

3. EXPERIMENTS AND DATA REDUCTION

The experiments have been performed for a single tip-speed ratio: $\lambda = 5.1$; the tunnel-wind velocity is kept at $U = 4.5$ m/s, the speed of revolutions (≈ 35 Hz) is adjusted to match the tip-speed ratio.

For two pitch angles: $\theta_{tip} = +1.3^\circ$ and -2.7° , axial traverses have been made at $r/R = 0.5$ and 0.8 from $z/R = 0.08$ to 0.14 with increments of 0.02 and a radial traverse has been made at $z/R = 0.1$ from $r/R = 0.4$ to 1.0 with increments of 0.05 . A total of 40 runs are performed in this session.

For each position in a traverse a velocity sample is taken of both wires every 0.5° azimuth angle of the rotor over 4 successive revolutions. For each azimuth angle these 4 measurements are reduced to a mean, a minimum and maximum value, as shown in fig. 3.a,b,c, as examples.

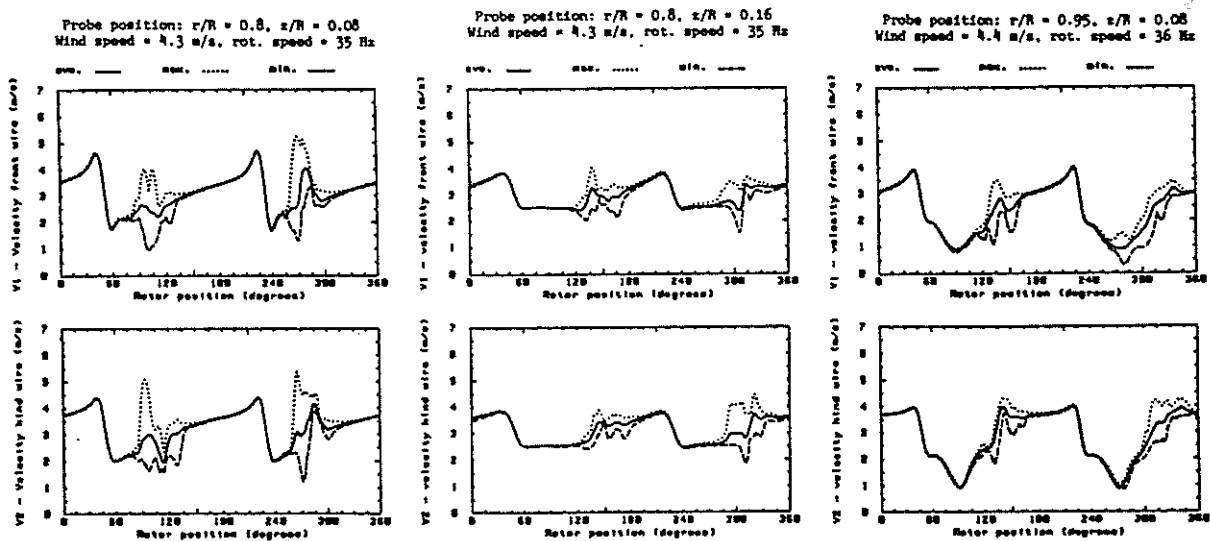


Figure 3.a,b,c Examples of a measurement

3.1 Interpretation of the measured data

Three striking features are clearly visible: a fast, but consistent fluctuation, near the tip followed by a local decrease and a region with a stochastic character.

The azimuthal position of the fast fluctuation, which coincides with the blade passage, does not change with the axial position of the probe. The magnitude of the fluctuation however decreases with the distance to the

rotor plane (see fig. 3.b). This leads to the assumption that this fluctuation is a direct result of the bound circulation on the blade.

The local decrease, which becomes stronger when approaching the wake boundary (see fig. 3.c), is attributed to the tipvortex.

The azimuthal position of the stochastic region changes with the axial position of the probe: with increasing distance from the rotor plane this region is detected at a higher azimuth angle (i.e. at a later time), see fig. 3.b. It is very likely that this region is the result of the vorticity sheet induced by the blade.

These phenomena in the azimuthal variation of the velocity have also been observed by De Vries and Den Blanken [4], but it was not the object in their research and little time was spend to interpret the data correctly.

3.2 A simple mathematical simulation

To validate the assumptions, a simple model has been set up, in a similar way as Surendraiah [5]: the blade is represented by a potential vortex, which implies:

$$V = \frac{\Gamma}{2\pi r} \dots\dots (1)$$

For a NACA 0012 aerofoil Wood and Westphal [6] showed that outside $z/c = 0.3$ the induced velocities can be calculated accurately by replacing the aerofoil with a vortex line at the quarter-chord position. In the underlying experiments axial traverses have been made from $z/R = 0.08$, which means $z/c \geq 0.4$ at $r/R = 0.5$ and $z/c \geq 0.5$ at $r/R = 0.8$, thus sufficiently far away from the aerofoil to yield bound vorticity velocities.

A series of potential vortices on a straight line in a parallel flow is taken. When traversing along the middle two vortices, the resultant of the parallel flow and the induced velocities of all the vortices gives the pattern as shown in fig. 4.

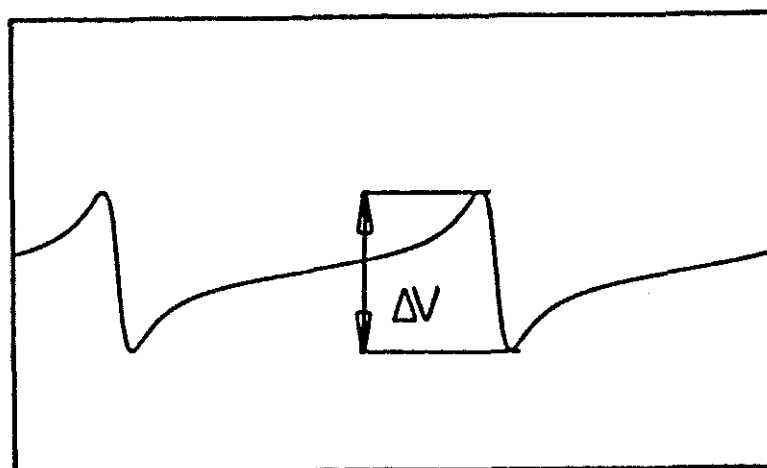


Figure 4. Mathematical simulation

When only the axial component is taken, the influence of the vortex ΔV , appears to be proportional to the circulation Γ and inversely proportional to the axial distance z . The absolute distance from the probe to the rotor plane is not exactly known, but the incremental steps in z -direction have been taken accurately. Because we are only interested in the slope of the curve, it is best to take the reciprocal of the inverse gradient. The circulation is therefore calculated from:

$$\Gamma = 2\pi * \left\{ \frac{\partial(1/\Delta V)}{\partial z} \right\}^{-1} \dots\dots (2)$$

3.3 Testresults

When linear regression is applied to the reduced data of the axial traverses the following result for the circulation is obtained (see also fig. 5):

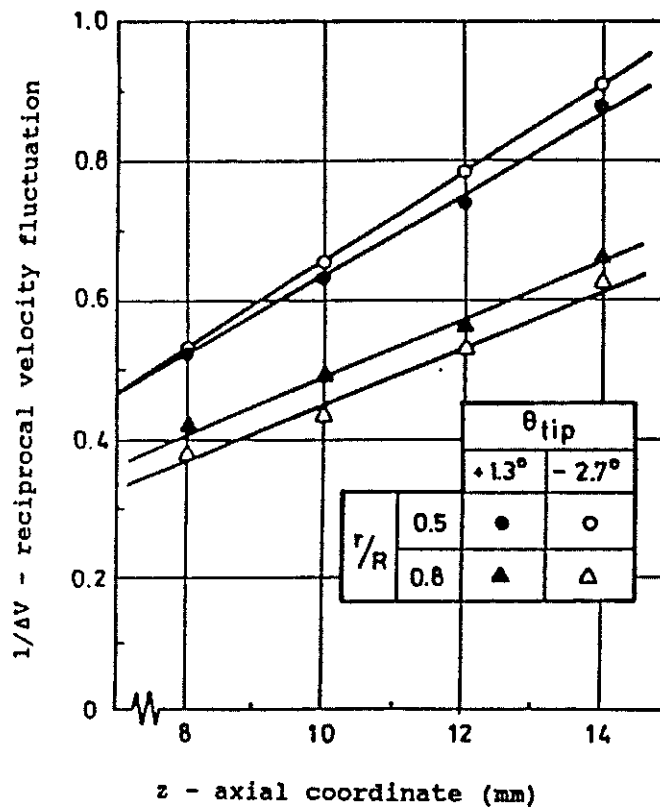


Figure 5. Linear regression on reduced data

TABLE 1 - Circulation on the rotating blade at two radial stations.

Γ (m^2/s)		θ_{tip}	
		+1.3°	-2.7°
r/R	0.5	0.107	0.099
	0.8	0.157	0.137

The reduced data of the radial traverses show the relative circulation distribution over the blade (fig. 6).

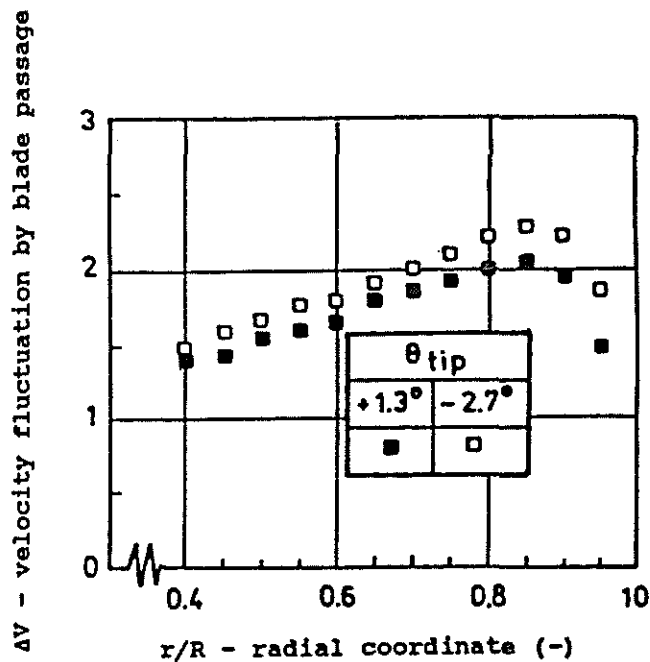


Figure 6. Relative span-wise circulation distribution

The higher values for $\theta_{tip} = -2.7^\circ$ in this plot do not necessarily mean a higher circulation. The circulation can not be determined from a single measurement, but only from the gradient of $1/\Delta V$ in axial direction.

3.4 An unsolved curiosity

Inside the rotor wake the tipvortex gives a local decrease, outside the wake a local increase of the velocity. Unfortunately, this last situation was not included in this session. In an earlier session, when no data acquisition system was available, this has been observed on a oscilloscope and led to an until now unsolved curiosity.

By positioning the probe close to the outside of the wake boundary the influence of the passage of the tipvortex is very clear by a local increase in velocity. By monitoring the pulse from the opto-coupler, the time from rotor plane to the detection of the tipvortex can be determined. This is done for several axial distances of the probe to the rotor plane. In a plot of distance versus time the measuring points give a straight line and the slope, dx/dt , is the transport velocity of the helical vortex system. This velocity (3.4 m/s) deviates significantly from the local velocity between the detection of the vortices (4.0 m/s), which was also read from the oscilloscope.

During visualization of the tipvortex path by smoke injection, it is observed that the tipvortices have each their own transport velocity. When the two blades were set to a different pitch angle, one helical path was slower and was, after approximately 3 rotations, overtaken by the other, so the helicals became entwined. Similar observations have been made by Alfredsson and Dahlberg [7] and [8].

4. THE COMPUTER CODES VIAX AND PREDICHAT

The simple mathematical simulation described in paragraph 3.2 shows that the fast fluctuation in velocity during the passage of the blade along the probe can be attributed to a discrete bound vortex.

There is however a more sophisticated model in operation at the Institute for Windenergy, which is to a large extent comparable to a (three dimensional) lifting line approach.

The roots of this model were already developed in 1980. An overview of the state of the art at that moment (related to a tipvane windturbine model) was published at the AGARD Conference on Prediction of Aerodynamic Loads on Rotorcraft (Van Bussel et al. [9]).

In a later stage a performance and load prediction code was defined, designated PREDICHAT (Van Bussel [10]). For the purpose of the present research it was decided to extend the model towards the possibility of calculating axial velocities at any desired location in the wake of the rotor. The computer code in which this possibility is taken into account is designated VIAX.

4.1 The theory behind the codes

Both PREDICHAT and VIAX are based upon the acceleration potential approach. Furthermore a matched asymptotic expansion technique is used for the derivation of the model. In PREDICHAT a viscous routine is added, in order to take into account the viscous drag of the airfoils, and to limit the maximum attainable lift coefficient according to measured two dimensional data loads. In VIAX viscosity is not taken into account.

With the asymptotic expansion technique it is possible to develop models with an increasing order of accuracy. For both PREDICHAT and VIAX first order models are used. This means that these models are in the far field equivalent to lifting line models. In the near field the model uses the pressure distribution of a flat plate aerofoil.

The acceleration potential approach assumes small disturbances in the velocity field. In principle this small perturbation assumption is not applicable for wind turbines: with simple momentum theory it can be derived easily that the optimum point of operation of a windturbine (for maximum

performance) is related to a reduction of the wind speed with 33 % in the rotor plane!

However it is also known that for a number of applications the resulting model is rather well applicable in the not-so-small-perturbation situation.

4.2 Delinearisation

For PREDICHAT it turned out to be necessary to include an extra iteration step in the procedure, in order to obtain acceptable results. The iteration step concerns the velocity with which the particles are travelling towards the rotor.

In linearized theory it is assumed that this speed is constant, and equal to the undisturbed wind velocity (this straight unperturbed path however is not consistent with the pressure distribution on the rotor blade). Accelerations are then found along this straight constant velocity path, so they can be integrated to yield a perturbed velocity at the rotor blade (its value dependent upon the position along the rotor blade).

The extra iteration uses the calculated velocity at the blade in the first iteration as the (constant) travelling speed in the second iteration. This results in a considerable modification of the calculated loads, without having a significant effect upon the calculated perturbed velocity. This approach can be made plausible with some reasoning: the small perturbation assumption is critical in the region close to the rotor blade. In the not so small perturbation situation (as with a windturbine near the optimal performance point of operation) the difference between the undisturbed wind velocity and the actual velocity is considerable.

In the second iteration the perturbations from the "undisturbed velocity" (taken equal to the calculated velocity at the rotorblade in the first iteration) are small! The model is now equivalent to a lifting line model (in the far field), with an axial perturbation of the "helical" vorticity sheet in such a way that the speed at which the sheet travels along the wake varies with the radial position.

The wake, and thus the vorticity sheet are not assumed to have a radial velocity component. So wake divergence (the normal wind turbine situation) is not taken into account.

4.3 Validation

Comparison of PREDICHAT predictions with the predictions of other methods, and with experiments showed that this acceleration potential method is as good as the others for performance predictions, fig.1. See Van Bussel and Van Kuik [1]) and Van Bussel [10] for more comparisons.

For the calculation of the velocities in the wake an approach is used similar to the iteration process for the rotor blade velocities. In a first iteration a disturbed velocity is calculated at the considered point, and this (perturbed) velocity is taken as the traveling velocity in the second iteration. This approach, made operational in VIAX, has not yet been validated; the present paper shows a first attempt to it.

5. COMPARISON BETWEEN MEASUREMENTS AND NUMERICAL RESULTS

For the blade pitch angle $\theta_{tip} = -2.7^\circ$ a number of prediction have been performed for the velocities in the wake.

Although the same values have been chosen as in the experiment for the radial and the axial positions, they can not be compared directly. There are a number of reasons for the inability of a direct comparison.

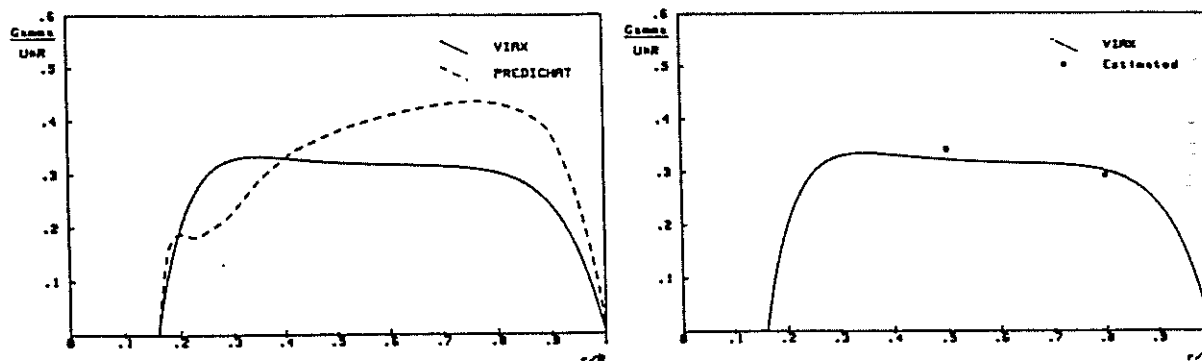
At first it was noticed in the experiments (by means of flow visualization with smoke) that there is a severe flow separation along the nacelle of the rotor (see also paragraph 2.2). This separation is not be incorporated in present codes PREDICHAT and VIAX.

In the second place it is unknown what the two dimensional characteristics are of the curved plate aerofoils used on the model (typical Reynoldsnumber $Re = 20.000$). So the aerodynamical characteristics used in the codes (such as $dCl/d\alpha$ and zero lift angle α_0 for both codes and the polar curve for PREDICHAT) had to be estimated.

Still the results obtained by now from the codes give confidence in the interpretation of the measurements, and are promising for further use, as will be shown.

At first the predicted power curve ($C_p - \lambda$ curve) with PREDICHAT showed good agreement with the measured $C_p - \lambda$ data.

In figure 7 the corresponding load distribution (in terms of a non dimensionalized Γ distribution) for a tip-speed ratio $\lambda = 5.1$ is depicted.



Gamma-distribution over the rotorblade.

Configuration THE_2_4_28 Aerofoil: GEN_PL68
 Lambda 5.1 Blade tip pitch -2.7 degr.

Figure 7. Calculated circulation distributions for $\lambda = 5.1$ and estimations resulting from wake velocity variations

Apart from the prediction originating from PREDICHAT (which includes the effects of viscosity to a certain extend), also the VIAX prediction (inviscid) is depicted. The discrepancy in the root region is clearly evident. This is a common feature in wind turbine rotor aerodynamics, and can be understood when it is realized that near the hub the oncoming flow angle increases towards 90 degrees (perpendicular to the rotorplane) at zero radius. The blade designs always have a (very) limited amount of twist thus resulting in large angles of attack in the root section. Inviscid theory (VIAX) calculates loads according to $Cl = Cl_{\alpha} \cdot \alpha$, whereas PREDICHAT assumes a maximum Cl equal to the measured value in two dimensional experiments.

Also the Cl_{α} used in PREDICHAT is taken from two dimensional data. The scarce data available showed that in the higher Cl regions a Cl_{α} can be expected well above 2π . This results in higher predicted Γ -values with PREDICHAT in the middle and the tip region of the rotor blade.

From fig.7 it thus becomes clear that the calculated velocities in the wake (with the inviscid code VIAX) will differ from the experimental values (for which a load distribution equivalent to the PREDICAT prediction is assumed).

Figure 8 shows some calculated axial velocity variations with the azimuthal position. The blades are present at 0 and 180 degrees.

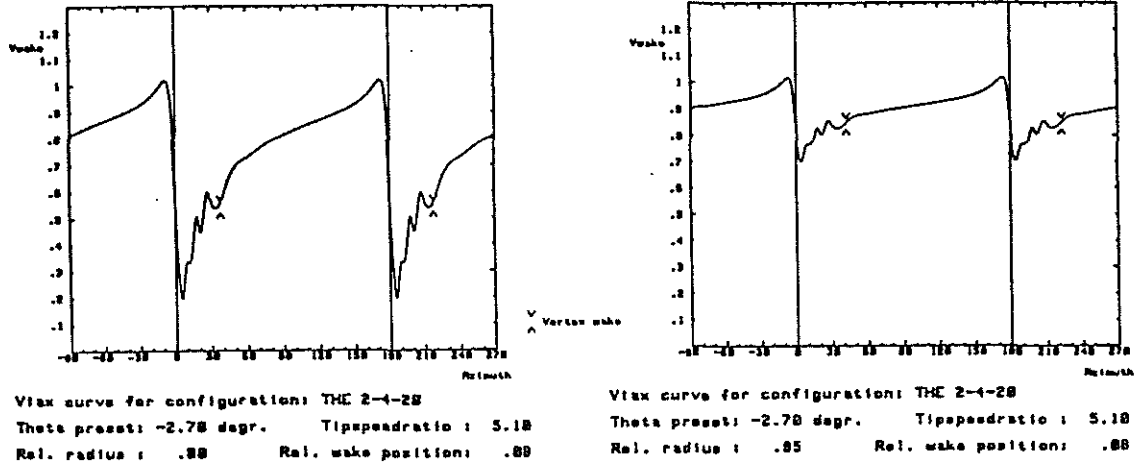


Figure 8. Non-dimensional axial velocities at $z/R = 0.08$, calculated with VIAX

The general picture is quite similar to those from the experiments summarized in fig.3. The position of the vortex wake is calculated under the assumption that the (local) convection velocity determined in the rotorplane stays constant during the travel to the considered axial position.

In figure 9 the effect of variation of the axial position upon the velocity distribution is depicted.

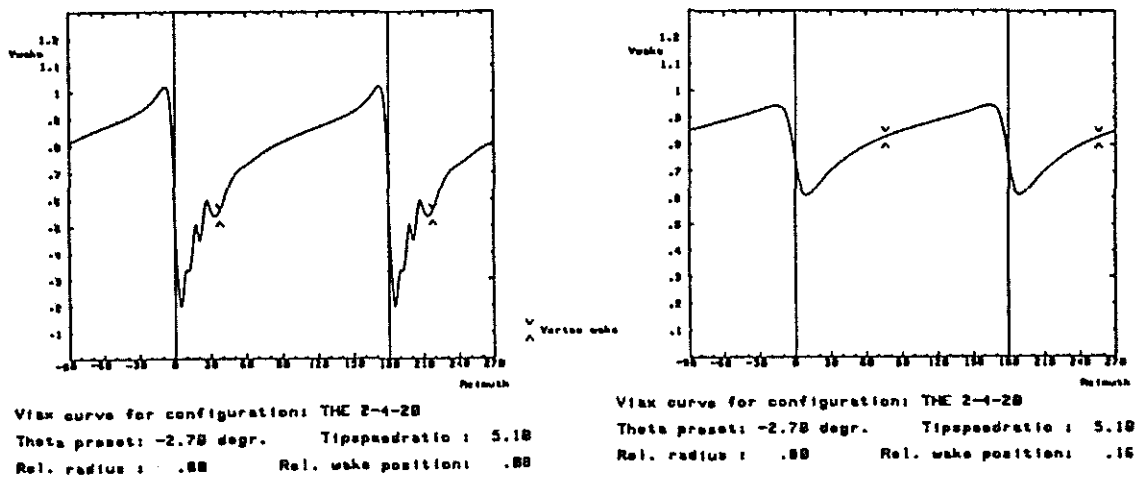


Figure 9. Variation of the calculated non-dimensional wake velocities with the axial distance behind the rotor

Just as in figure 3 it can be seen clearly that the fast fluctuation of the velocity around $\psi = 0^\circ$ and $\psi = 180^\circ$ decreases in intensity with increasing axial distance.

In the paragraphs 3.2 and 3.3 a method is proposed for deriving the local value for the circulation from the measured peak-peak value of the fast fluctuation.

In the theoretical model this approach can be validated because the local Γ value estimated from the velocity fluctuation can be compared with the "actual" Γ value, which is known in the theoretical model. The result is shown in fig. 7.

From this comparison it can be seen that it seems indeed very well possible to determine the local value of the circulation at the rotor blade from the measured velocity pattern in the very near wake!

6. CONCLUSIONS

By fast sampling of a hot-wire signal, it is possible to obtain detailed information on the velocity distribution in the wake of a rotor model. Global measurements would give a distorted impression of the velocity distribution in the rotor wake: the velocity fluctuations generated by the blade passages would be misinterpreted as being turbulence. It is however a well-determined signal. The influence of the tip vortex has a strong influence on the averaged velocity near the wake boundary, but this is a local phenomenon.

It seems possible to determine the circulation distribution on a rotating blade, by interpreting the detailed near-wake measurements in an adequate way. The simulation in the theoretical model of this approach shows its potentials. It indicates that the local circulation can indeed be deduced very accurately from the velocity fluctuation in the wake.

With the described measurements, it is possible to verify prediction codes which have the same degree of detailing, such as codes based on the acceleration potential method. The axial velocity distributions calculated with VIAX show a behavior similar to the measured characteristics.

More realistic experiments with a larger rotor (higher Re number), with well-known aerofoils are planned. In the absence of massive flow separations and with a limited stall area it may even be possible to obtain a quantitative agreement with experimental results.

An attempt will be made to set up an arrangement to deduce the three velocity components. By further detailing, a progress in physical insight can be obtained. It has been shown that the velocity field is far from uniform and so will the related pressure field be.

To verify prediction codes, which use the laws of energy and momentum conservation, detailed pressure measurements will have to be done to complete the experimental data.

REFERENCES

1. G.J.W. van Bussel and G.A.M. van Kuik, "Rotoraerodynamica van horizontale-as windturbines, NEWIN-workshop d.d 16-4-1985", IW-R505, Institute for Windenergy, Delft University of Technology, Delft, The Netherlands, 1985. (in Dutch)
2. P.D. Clausen and D.H. Wood, "An experimental investigation of blade element theory for wind turbines. Part 2. Phase-locked averaged results", Journal of Wind Engineering and Industrial Aerodynamics, 31, 1988.
3. P.D. Clausen et al., "An experimental investigation of blade element theory for wind turbines. Part 1. Mean flow results", Journal of Wind Engineering and Industrial Aerodynamics, 25, 1987.
4. O. de Vries and N.H.G. den Blanken, "Second series of wind-tunnel tests on a model of a two-bladed horizontal axis wind turbine", NLR TR 810698L, Nationaal Lucht- en Ruimtevaart Laboratorium, Amsterdam, The Netherlands, 1981.
5. M. Surendraiah, "An experimental study of rotor blade-vortex interaction", NASA CR-1573, 1970.
6. D.H. Wood and R.V. Westphal, "Measurements of the flow around lifting-wing/body junction", Submitted to AIAA Journal, 1988.
7. P-H Alfredsson and J-A Dahlberg, "A preliminary wind tunnel study of windmill wake dispersion in various flow conditions", AU-1499, Part 7, FFA, Bromma, Sweden, 1979.
8. P-H Alfredsson and J-A Dahlberg, "Measurements of wake interaction effects on the power output from small wind turbine models", HU-2189, Part 5, FFA, Bromma, Sweden, 1981.
9. G.J.W. van Bussel, Th. van Holten, G.A.M. van Kuik, "Aerodynamic Research on Tipvane Windturbines", AGARD-CP 334, 1982.
10. G.J.W. van Bussel, "First order performance calculations of windturbine rotors using the method of the acceleration potential", IW-R522, Institute for Windenergy, Delft University of Technology, Delft, The Netherlands, 1989.